Corrosion Science 124 (2017) 131–137

Contents lists available at ScienceDirect

Corrosion Science

journal homepage: www.elsevier.com/locate/corsci

Microstructure evolution and high-temperature mechanical properties of SiC_f/SiC composites in liquid fluoride salt environment

Hongda Wang[a,b,c], Qian Feng[d], Zhen Wang[a,b], Haijun Zhou[a,b,*], Yanmei Kan[a,b], Jianbao Hu[a,b], Shaoming Dong[a,b,*]

[a] State Key Laboratory of High Performance Ceramics and Superfine Microstructure, Shanghai Institute of Ceramics, Chinese Academy of Sciences, Shanghai 200050, China
[b] Structural Ceramics and Composites Engineering Research Center, Shanghai Institute of Ceramics, Chinese Academy of Sciences, Shanghai 200050, China
[c] University of Chinese Academy of Sciences, Beijing 100049, China
[d] Analysis and Testing Center, Donghua University, Shanghai 201600, China

ARTICLE INFO

Keywords:
A. Ceramic matrix composites
A. Molten salt
B. SEM
B. XRD
C. Exfoliation corrosion
C. High temperature corrosion

ABSTRACT

High temperature mechanical properties and microstructure evolution of chemical-vapor-infiltrated SiC fiber reinforced SiC ceramic matrix composites (SiC_f/SiC) in 46.5LiF-11.5NaF-42.0KF (mol.%, FLiNaK) eutectic salt were investigated. The results indicate that the corrosion of SiC_f/SiC composites was accelerated with increase of corrosion temperature. Interlayer boundaries in SiC matrix with higher oxygen content were corroded preferentially. The F^- formed Si—F coordinate bond with SiC and replaced carbon, followed by the corrosion of SiC matrix. While single SiC fiber tensile strength suffered no depravation after corrosion, corrosion and damage of SiC matrix led to deteriorated high temperature mechanical properties of SiC_f/SiC composites.

1. Introduction

Silicon carbide (SiC) continuous fiber-reinforced SiC matrix composites (SiC_f/SiC) have a multitude of excellent properties, including high temperature mechanical performance with better mechanical damage tolerance over inherently brittle monolithic SiC [1,2], outstanding thermal conductivity, low activation to neutron-induced radioactivity [3–7], which make the SiC_f/SiC composites a promising candidate material for structural and functional components in nuclear reactors. Particularly, SiC_f/SiC composites have nice compatibility with liquid fluoride salt (e.g. 46.5 mol% LiF- 11.5 mol% NaF-42.0 mol% KF eutectic molten salt, i.e. FLiNaK molten salt). This unique properties of SiC_f/SiC composites make it achieve wide attention due to their potential application in heat-exchanger, control rod and other structure components in Molten Salt Reactor (MSR) [8–11]. However, SiC undergoes corrosion in liquid fluoride salt at high temperature because of the disequilibrium in thermodynamics between SiC and fluoride salt [11]. Obviously, the corrosion of SiC compromises the advantages of SiC_f/SiC composites in nuclear application. The corrosion behavior of SiC_f/SiC composites in liquid fluoride salt has been seldom investigated up to now, especially the evolution of microstructure and mechanical performance.

It is indicated that the impurities in fluoride salt and the composition of SiC-based materials lead to the incompatibility of SiC_f/SiC composites to fluoride salt. The foreign ions (i.e. Ni^{2+}, Cr^{2+} and Cr^{3+}), which could be introduced during production of fluoride salt or by corrosion of Hastelloy N alloy, can accelerate the corrosion of SiC [12,13]. Although the reason of optionally corrosion of SiC is still unknown, qualitative explanation with the respect of the standard Gibbs free energy of fluoride formation per F_2 molecule of the Si and SiC phases has been widely accepted [14]. The Si—O bond in O-contained SiC phase would be attacked by F^- to form Si—F bond, indicating that the oxygen in SiC accelerates the corrosion of SiC in fluoride salt [15]. Therefore, high-purity SiC is needed in nuclear reactor application.

There is a variety of technology for preparing SiC_f/SiC composites, such as nano-infiltration and transient eutectic phase [16], polymer impregnation and pyrolysis [17], reaction sintering [18] and chemical vapor infiltration (CVI) process [19]. Among these methods, the CVI process could form highly crystalline, near-stoichiometric SiC matrix and minimize damage of fibers during material fabrication, which are beneficial to produce the nuclear grade SiC_f/SiC composites [20]. However, few research has focused on the corrosion behavior of CVI SiC_f/SiC composites and mechanical performance in liquid fluoride salt environment.

---

[*] Corresponding authors at: State Key Laboratory of High Performance Ceramics and Superfine Microstructure, Shanghai Institute of Ceramics, Chinese Academy of Sciences, Shanghai 200050, China

E-mail addresses: zhouhj00000@mail.sic.ac.cn (H. Zhou), smdong@mail.sic.ac.cn (S. Dong).

http://dx.doi.org/10.1016/j.corsci.2017.05.016
Received 10 September 2016; Received in revised form 16 May 2017; Accepted 23 May 2017

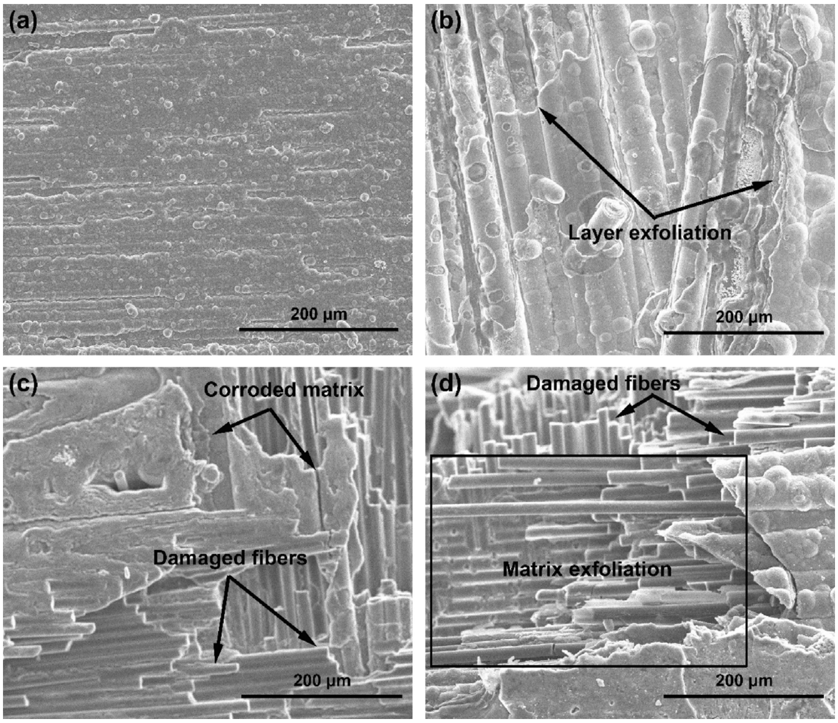

Fig. 1. Surface SEM images of SiC_f/SiC composites (a) before corrosion and after corrosion in liquid FLiNaK salt at (b) 800 °C, (c) 900 °C and (d) 1000 °C for 500 h.

In this work, the static corrosion behavior of CVI SiC_f/SiC composites in molten FLiNaK salt at various temperature was studied. The microstructure evolution during the corrosion process, and the high temperature mechanical properties were investigated.

2. Experimental

The materials used to evaluate corrosion behavior are SiC matrix composites reinforced by two-dimensional woven fabrics of KD-II SiC fibers (National University of Defense Technology, Changsha, China). Using the Methyltrichlorosilane (MTS) as the raw material and H_2 as the carrier gas, the SiC_f/SiC composites were prepared via CVI processing. Prior to the CVI process, a pyrolytic carbon (PyC) monolayer of ~100 nm in thickness was deposited on the SiC fiber surface through chemical vapor deposition. The fiber volume fraction, porosity and density of the as-received composites were ~40%, ~5.01% and 2.74 $g \cdot cm^{-3}$, respectively. The monolithic composites were machined into $35 \times 4 \times 2\ mm^3$ bar for the corrosion experiment. Each test group contained 5 bars.

According to the design goals of Generation IV reactors, the outlet temperature of MSR would be 700 °C–800 °C [21], and the peak temperature of Advanced High Temperature Reactor would be up to 1000 °C [11]. To evaluate the performance of SiC_f/SiC composites in the similar environment in reactor, 800 °C, 900 °C and 1000 °C were chosen as the corrosion temperature, and the corrosion time was 500 h [22]. The SiC_f/SiC composites samples were transferred into a glove box under the protection of high purity argon gas. The atmosphere in the glove box was controlled at $O_2 < 0.1$ ppm and moisture < 0.1 ppm all along. Before corrosion, the graphite crucible and SiC_f/SiC samples were heat-treated in furnace in the glove box at 700 °C for 10 h to eliminate possible adsorption of air and other gases. Subsequently, SiC_f/SiC samples were fixed on a graphite support and dipped into ~80 g 46.5LiF-11.5NaF-42.0KF (mol.%, FLiNaK) fluoride eutectic molten salt (Shanghai Institute of Organic Chemistry, Chinese Academy of Sciences, Shanghai) in the graphite crucibles. The same SiC fibers used in SiC_f/SiC composites were also introduced into the crucibles at the same time to study the effect of corrosion on mechanical properties of SiC fibers. And then, the crucibles were heated to 800 °C, 900 °C or 1000 °C for 500 h, respectively. After the high temperature corrosion process in fluoride eutectic molten salt, the SiC_f/SiC composite samples were picked out from the crucible and immersed into $1\ mol \cdot L^{-1}$ $Al(NO_3)_3$ solution to remove the fluoride salt solid adhered on the exterior and interior surfaces of the sample [23]. Finally, the samples were washed with deionized water using an ultrasonic cleaner, and then dried at 120 °C in a vacuum drying chamber.

The samples were weighed by precision balance (BT-25-S, 0.01 mg, Sartorius) before and after the corrosion test, and the mass loss ratio was calculated to characterize the corrosion resistance of the composites. Every bar in each test group was measured 3 times independently to obtain the mass loss ratio and mass loss rate of each bar. Then data of 5 bars in each experiment group was used to calculate the average mass loss ratio, mass loss rate and the corresponding standard deviation. The mass loss ratio (m_l) could be calculated by the formula below:

$$m_l = \frac{m_0 - m}{m_0} \times 100\% \tag{1}$$

where m_0 and m are the mass of sample before and after corrosion, respectively. The apparent mass loss rate (v) was introduced to semi-quantitatively describe the corrosion rate:

$$\nu = \frac{m_0 - m}{S \cdot t} = \frac{m_0 - m}{2(LH + LW + HW) \cdot t} \tag{2}$$

where S is surface area of sample, t is corrosion time, and L, W, H are the length, width, height of sample, respectively. Phase compositions of the samples were analyzed by X-ray diffraction (XRD, D8 Advance, Bruker AXS Co. Ltd., GER) at room temperature, using Cu Kα radiation ($\lambda = 0.154$ nm) 2θ over the angles range of 10°–80°. High temperature flexural strength of the samples after corrosion was measured through a three-point-bending test (Instron-5500R, Instron Corp., Canton, USA) with a span of 30 mm and a loading rate of 0.5 mm/min in air atmosphere. For a comparison, the high temperature flexural strength of samples without corrosion was also measured. 3 bars were tested for each group. Polished cross-section and surface morphologies of the samples before and after corrosion at varying temperatures were characterized by scanning electron microscope (SEM, Quanta-250, FEI, USA) along with energy dispersive spectrometer (EDS, Oxford, UK). Additionally, the single fiber tensile strength of SiC fibers before and